Journal of Hazardous Materials 174 (2010) 746–755

Contents lists available at ScienceDirect

Journal of Hazardous Materials

journal homepage: www.elsevier.com/locate/jhazmat

Adsorptive performance of un-calcined sodium exchanged and acid modified montmorillonite for Ni^{2+} removal: Equilibrium, kinetics, thermodynamics and regeneration studies

Christianah Olakitan Ijagbemi, Mi-Hwa Baek, Dong-Su Kim*

Department of Environmental Science and Engineering, Ewha Womans University, Daehyundong 11-1, Seodaemungu, Seoul 120-750, Republic of Korea

ARTICLE INFO

Article history:
Received 3 July 2009
Received in revised form 28 August 2009
Accepted 22 September 2009
Available online 30 September 2009

Keywords:
Na-montmorillonite
A-montmorillonite
Nickel
Adsorption
Regeneration

ABSTRACT

The efficacy of un-calcined sodium exchanged (Na-MMT) and acid modified montmorillonite (A-MMT) has been investigated for adsorptive removal of Ni^{2+} from aqueous solution. Physico-chemical parameters such as pH, initial Ni^{2+} concentration, and equilibrium contact time were studied in a series of batch adsorption experiments. The equilibrium time of contact for both adsorbents was about 230 min. The Redlich–Peterson model best described the equilibrium sorption of Ni^{2+} onto Na-MMT and the Dubinin–Radushkevich model was the best model in predicting the equilibrium sorption of Ni^{2+} onto A-MMT. The kinetics of Ni^{2+} uptake by Na-MMT and A-MMT followed the pseudo second-order chemisorption mechanism. Sorptions of Ni^{2+} onto Na-MMT and A-MMT were spontaneous and endothermic. Regeneration was tried for several cycles with a view to recover the adsorbed Ni^{2+} and also to restore Na-MMT and A-MMT to their original states. The un-calcined Na-MMT and A-MMT have adsorptive potentials for removal of Ni^{2+} from aqueous bodies.

1. Introduction

The most fundamental challenge of this age is to have a benign environment with less toxic substances. In the industrialized world, less than 10% of inputs (raw materials) into a manufacturing process do show up in the final product. 90% end up as waste and often times as effluents from which toxic heavy metals such as nickel, copper, lead, zinc, iron, mercury, chromium, tin and cadmium are released as pollutants into the environment [1]. Waste discharge from zinc base casting, battery storage, silver refineries, and electroplating industries do present Ni^{2+} as part of their major constituents. Nickel is harmful if discharged in appreciable quantity to natural waters [2]. In India, the acceptable limit of Ni^{2+} in drinking water is 0.01 and 2.0 mg/L as industrial wastewater discharge [3], beyond these concentrations; Ni^{2+} may cause cancer of the lungs, nose and bone. Nickel itch, an allergy from contact with nickel coins and jewelries is another most frequent effect of Ni exposure. Nickel's acute poisoning may cause headache, dizziness, nausea and vomiting, chest pain, dry cough and extreme weakness [2,4].

Heavy metal ions are not bio-degradable; they are usually removed from contaminated water by physical or chemical treatment processes. Treatment processes for heavy metal contaminated waste effluents include, chemical precipitation, ion exchange, adsorption and ultra-filtration but the preference for a particular method is jointly based on the concentration of heavy metals in the solution, the cost of treatment and the market value of the process [5]. Removal of heavy metals from wastewater has mostly been characterized by adsorption process [5,6] particularly, when natural materials that are available in large quantities or certain waste products from industrial or agricultural activities may have potentials as inexpensive adsorbents [6]. Adsorption process is effective and efficient even at trace concentration of heavy metal ions. The drawback of the method is the high cost and tedious procedure for the regeneration of the convectional adsorbent (activated carbon). To overcome this disadvantage in the last few years, several approaches have been studied towards the development of new cost-effective substitutes from naturally occurring materials [5].

Montmorillonite (MMT), a member of the natural clay minerals has been studied for removal of heavy metal cationic species in aqueous bodies [7–9]. MMT can be modified in different ways to obtain specific chemical, surface, and structural properties for different applications by pre-treatment with chemicals or combined treatment such as heating and chemical attacks. Sodium salt treatment improves ion exchange efficiencies of MMT for heavy metal removal, and the distribution coefficient of cationic species on Na^+-exchanged MMT could be about two times that on Ca^{2+}-MMT [10]. Acid activation of MMT is another important process for modifying the physical and chemical properties of the clay and in

* Corresponding author. Tel.: +82 2 3277 2394; fax: +82 2 3277 3275.
E-mail address: dongsu@ewha.ac.kr (D.-S. Kim).

0304-3894/$ – see front matter © 2009 Elsevier B.V. All rights reserved.
doi:10.1016/j.jhazmat.2009.09.115

Nomenclature

q_t	amount of Ni^{2+} adsorbed per unit mass of adsorbent at any time t (mg/g)
q_e	adsorption capacity at equilibrium (mg/g)
C_e	equilibrium concentration of Ni^{2+} in solution (mg/L)
C_0	initial concentration of the Ni^{2+} solution (mg/L)
C_t	liquid-phase concentrations of the Ni^{2+} solution at any time t (mg/L)
V	volume of the Ni^{2+} solution (mL)
m_s	amount of sorbent used (g)
P/P_0	relative pressure
K_F	Freundlich isotherm constant related to adsorption capacity ((mg/g)(L/mg)$^{1/n}$)
K_L	intensity of adsorption (L/mg)
n_F	Freundlich isotherm constant related to adsorption intensity
Q_m	maximum adsorption at monolayer coverage (mg/g)
b	constant related to the extent of adsorption (L/mg)
R_L	dimensionless separation factor
R^2	correlation coefficient
b_T	Tempkin heat of sorption (kJ/mol)
B_T	Tempkin isotherm energy constant (dimensionless)
A_T	Tempkin adsorption potential (L/mg)
Q_{DR}	D–R adsorption capacity (mg/g)
γ	D–R adsorption energy constant (mol^2/kJ^2)
ε	Polanyi potential
E	sorption energy (kJ/mol)
K_R	constant of Redlich–Peterson
A_{RP}	constant of Redlich–Peterson
β	Redlich–Peterson heterogeneity index
R	gas constant (J/(mol K))
K_D	distribution coefficient
T	absolute temperature (K)
t	time (min)
ΔG°	change in Gibb's free energy of adsorption (kJ/mol)
ΔH°	change in enthalpy of adsorption (kJ/mol)
ΔS°	change in entropy of adsorption (kJ/mol K)

turn determines its potential for different applications [11]. During acid attack, the exchangeable cations are initially replaced by protons, followed by partial dissolution of the tetrahedral and octahedral sheets leading to creation of new acid sites in the structure and thereby making the clay more porous [12]. Modified MMT are important because, among other uses, they have potential application in the disposal of other hazardous and nuclear wastes [13].

Considering the large deposits of clay minerals and their physico-chemical properties as adsorbents, detailed kinetic, isotherm, thermodynamic and regeneration studies were carried out to investigate the heavy metal removal potentials of uncalcined Na-MMT and A-MMT in aqueous medium using Ni^{2+} as a representative of the heavy metal cationic species.

2. Experimental

2.1. Materials

Montmorillonite K 10 (MMT) and other chemicals used in the study were purchased from Aldrich Chemicals. Na-MMT was prepared by treating MMT with 10% (w/v) of 1 M of NaCl solution under mechanical stirring for 24 h at ambient temperature. This procedure was repeated five times in order to attain maximum saturation as this process gives effective saturation of sodium ions compared to those using higher concentration of the solution with shorter contact time. After activation the clay fractions were separated from the solution by centrifugation and washed with distilled water until sample was free of Cl^- using 0.01 M $AgNO_3$ drop on the supertant [14] and later dried at 105 °C for 6 h. Portions of MMT were equally subjected to acid treatment by refluxing in a shaking water bath with 10 g of MMT dispersed in 400 mL of 8 N H_2SO_4 solution, the resulting suspension was aged for 3 h at 90 °C followed by washing with distilled water till sample was SO_4^{2-} free using 0.01 M $BaCl_2$ drop on the supertant [14,15]. The achieved A-MMT sample was also dried at 105 °C for 6 h. Both clay fractions (Na-MMT and A-MMT) were each powdered and passed through a 150 μm sieve.

2.2. MMT characterization

Physico-chemical characterization of MMT, Na-MMT and A-MMT were carried out using standard procedures. Specific surface area was determined by Braunauer–Emmett–Teller (BET) nitrogen adsorption technique using surface area and porosimetry analyzer (Micromeritics - TriStar 3020 Gas Adsorption Analyzer). X-ray diffractograms (XRDs) were obtained with Philips 3020 diffractometer operating at 40 kV and 30 mA and using Cu-Kα radiation (λ = 1.5405 scanning speed of 1° (2θ) min^{-1} from 2° to 70° (2θ)). The IR spectra of the samples were recorded in the region 4000–600 cm^{-1} on a Jasco FT-IR spectrometer at 4 cm^{-1} resolutions.

2.3. Adsorption studies

Stock solution of Ni^{2+} was prepared by dissolving an appropriate quantity of $Ni(NO_3)_2{\cdot}6H_2O$ in three times distilled water (>18 MΩ). The stock solution was diluted to 50, 75 and 100 mg/L to obtain the initial Ni^{2+} concentrations used in the sorption experiments. Equilibrium experiments were carried out by contacting 0.3 g from each of the adsorbents with 50 mL of Ni^{2+} solution at different initial concentrations. For optimization of experimental conditions like temperature, adsorbate concentration and contact time, batch experiment were performed with the sorbent–sorbate suspension in a 100 mL conical flask, at 25 °C and 200 rpm in a mechanical shaking incubator equipped with a temperature controller. To examine the effect of temperature on the adsorption process, the temperature of the adsorbate solution was controlled between 15 and 45 °C. The effect of pH on the adsorption process was investigated by varying the pH of Ni^{2+} solution from 2.3 to 9.8. The pH of the solution was controlled with 0.1 M HCl and 0.1 M NaOH solution as per required pH value. After each reaction, aliquots of the treated samples were separated by filtration, followed by analysis of the filtrate for residual Ni^{2+} using PerkinElmer AAnalyst 300 Flame Atomic Absorption Spectrometer, according to standard methods for examination of water and wastewater [14,15].

The feasibility of Na-MMT and A-MMT reuse were assessed using desorption and regeneration processes. Desorption experiments were performed using 0.1 M HCl in a batch experimental study. The Ni^{2+} loaded Na-MMT and A-MMT were washed with deionised water, respectively, to remove any unadsorbed Ni^{2+}. The spent Na-MMT and A-MMT were then re-suspended in 50 ml of 0.1 M HCl following the same equilibrium condition for the adsorption process. The solution mixture was filtered and the adsorbent washed several times with distilled water in order to remove excess acid. It was then treated with 50 ml of Ni^{2+} solution and the above procedure was repeated for three cycles using the same adsorbents. All experiments were carried out in duplicate or triplicate with the mean of the results reported. The isotherm, kinetic and thermodynamic studies for the two adsorption processes were investigated under optimized conditions of reaction time.

3. Theory

3.1. Adsorption

The amount of Ni^{2+} adsorbed q_t (mg/g) at each time t, by Na-MMT and A-MMT can be calculated from the mass balance expression:

$$q_t = \frac{(C_0 - C_t)(V/1000)}{m_s} \quad (1)$$

and the percentage removal of Ni^{2+} can be obtained using Eq. (2):

$$Ni^{2+}\ \text{removal}\,(\%) = 100\left(\frac{C_0 - C_t}{C_0}\right) \quad (2)$$

3.2. Adsorption isotherm models

Acquired equilibrium data were fitted to different adsorption isotherm models in order to have insight into the sorption mechanisms, surface properties and affinities of Na-MMT and A-MMT for Ni^{2+} uptake.

3.2.1. Freundlich model

The Freundlich [16] adsorption isotherm has been interpreted as sorption to heterogeneous surfaces or surface supporting sites of different affinities. Freundlich assumption is that stronger binding sites are first occupied and as such, binding strength decreases with increasing degree of site occupation. The Freundlich model can be described as:

$$q_e = K_F(C_e)^{1/n_F} \quad (3)$$

The linear form of Freundlich model is given by:

$$\ln\ q_e = \ln K_F + \frac{1}{n_F}\ln C_e \quad (4)$$

A value of $1/n_F$ ranging between 0 and 1 (i.e. n_F is between 1 and 10) is a measure of surface heterogeneity and becoming more heterogeneous as this value gets closer to zero (0). If the value of n_F is below unity, it implies that the adsorption process is chemical, and if n_F is above unity, it is physical adsorption [17].

3.2.2. Langmuir model

The Langmuir [18] adsorption model is based on monolayer adsorption onto a homogeneous surface. Langmuir model assumes that adsorption forces are similar to the forces in chemical interactions. This model takes the form:

$$q_e = \frac{Q_m K_L C_e}{1 + K_L C_e} \quad (5)$$

Eq. (5) can be linearized as follows:

$$\frac{C_e}{q_e} = \frac{1}{bQ_m} + \frac{C_e}{Q_m} \quad (6)$$

Values of Q_m and b can be obtained from the plot of specific adsorption (C_e/q_e) vs. equilibrium concentration (C_e).

3.2.3. Tempkin model

The Tempkin and Pyzhev [19] model has a factor that explicitly describes the adsorbing species–adsorbent interactions by assuming a linear decrease in heat of adsorption with surface coverage. The model is mathematically represented as:

$$q_e = \frac{RT}{b_T}\ \ln(A_T C_e) \quad (7)$$

where

$$\frac{RT}{b_T} = B_T \quad (8)$$

The linear form of Tempkin model can be expressed as:

$$q_e = B_T\ \ln A_T + B_T \ln C_e \quad (9)$$

3.2.4. Dubinin–Radushkevich model

To further explain the physical and chemical characteristics of Na-MMT and A-MMT for Ni^{2+} uptake, the Dubinin–Radushkevich (D–R) isotherm was employed. The D–R isotherm, apart from being an analogue of the Langmuir isotherm; is more general than the Langmuir as it rejects the homogeneous surface or constant adsorption potential as expressed in Tempkin isotherm. The D–R model can be used to estimate the characteristic porosity of adsorbents and their apparent energy of adsorption. The model [20] is expressed in a linear form as:

$$\ln\ q_e = \ln Q_{DR} - \gamma\varepsilon^2 \quad (10)$$

ε is the Polanyi potential [21] expressed as:

$$\varepsilon = RT\ \ln\left(1 + \frac{1}{C_e}\right) \quad (11)$$

From the plot of $\ln q_e$ vs. ε^2 the values of γ and Q_{DR} can be determined. With the values of γ, the mean sorption energy (E) which is the free energy for the transfer of 1 mol of Ni^{2+} from infinity to the surfaces of Na-MMT and A-MMT can be calculated using Eq. (12):

$$E = (-2\gamma)^{-0.5} \quad (12)$$

3.2.5. Redlich–Peterson model

The Redlich–Peterson model is characterized by three adjustable parameters and provides better fit than the two-isotherm-parameter equations (Langmuir, Freundlich and Tempkin) that are more widely used. The Redlich–Peterson model [22] is given as:

$$q_e = \frac{K_R C_e}{1 + A_{RP} C_e^{\beta}} \quad (13)$$

3.2.6. Florry–Huggins model

Florry–Huggins isotherm model depicts the degree of surface coverage characteristic of the sorbate on the sorbent. The isotherm is expressed as [23]:

$$\log\frac{\theta}{C_0} = \log K_{FH} + \lambda\log(1 - \theta) \quad (14)$$

where $\theta = (1 - C_e/C_0)$ is the degree of surface coverage, K_{FH} is equilibrium constant, λ is the amount of Ni^{2+} occupying the active sites of the adsorbent.

3.3. Adsorption kinetics

Adsorption kinetics is one of the important characteristics defining the efficiency of an adsorbent. It describes the solute uptake rate which evidently controls the diffusion process and the residence time of adsorbate uptake at the solid–solution interface. Sorption kinetics can be controlled by several independent processes acting in parallel or in series. Such processes are external mass transfer (film diffusion), bulk diffusion, intraparticle diffusion and chemisorption (chemical reaction). To determine the solute uptake rate and explain the transport of Ni^{2+} to the surfaces of Na-MMT and A-MMT, different kinetic models were employed.

3.3.1. Pseudo first-order model

The Lagergren (pseudo first-order) rate equation is given by [24]:

$$\ln(q_e - q_t) = \ln\ q_e - k_1 t \quad (15)$$

where k_1 ($1\ \text{min}^{-1}$) is the rate constant of first-order adsorption.

3.3.2. Pseudo second-order model

The pseudo second-order model based on adsorption capacity and which equally agrees with chemisorption being the rate-controlling mechanism in adsorption processes was equally applied to the experimental data. Pseudo second-order model [25] is expressed as:

$$\frac{t}{q_t} = \frac{1}{k_2 q_e^2} + \frac{t}{q_e} \tag{16}$$

where k_2 (g/(mg min)) is the rate constant of second-order adsorption.

3.3.3. Elovich model

The Elovich equation is useful in describing adsorption on highly heterogeneous adsorbent. The Elovich [26] model is given by:

$$q_t = \frac{1}{\tau}\ln(\alpha\tau) + \frac{1}{\tau}\ln\ t \tag{17}$$

In the model, α is related to rate of chemisorption (initial adsorption rate) and τ is related to surface coverage (desorption constant).

3.3.4. Webber–Morris model

The Webber–Morris [27] model was equally employed; the initial rates of the Webber–Morris (intraparticle diffusion) model can be obtained by the linearization of Eq. (18):

$$q_t = k_{id} t^{0.5} \tag{18}$$

The intraparticle diffusion rate (k_{id}) constants for different initial Ni^{2+} concentrations can be obtained from the amount of Ni^{2+} adsorbed vs. $t^{1/2}$ plots.

3.4. Thermodynamic study

Thermodynamic parameters (Gibbs free energy, enthalpy and entropy) provide better understanding on the effects of temperature in adsorption processes. Generally, in physico-chemical reactions of which adsorption reactions are inclusive, the relationship between the distribution coefficient and temperature under the assumption that ΔH° is constant can be expressed by [28]:

$$\ln\ K_D = -\frac{\Delta H^\circ}{RT} + \frac{\Delta S^\circ}{R} \tag{19}$$

The distribution coefficient, K_D, can be defined as:

$$K_D = \frac{V}{m_s} \times \frac{C_0 - C_e}{C_e} \tag{20}$$

The value of ΔH° can be calculated from the slope of the plot of $\ln K_D$ vs. $1/T$ using Eq. (19). Other thermodynamic parameters such as ΔG° and ΔS° can be obtained from the calculated ΔH° using the following equations:

$$\Delta G^\circ = -RT \ln K_D \tag{21}$$

$$\Delta G^\circ = \Delta H^\circ - T\,\Delta S^\circ \tag{22}$$

4. Results and discussion

4.1. MMT characterization

XRD patterns of MMT reference standard and Na-MMT are typical for a natural and sodium-exchanged montmorillonite (Fig. 1). The main peak in the diffraction pattern of MMT ($2\theta \sim 7.2^\circ$) can be attributed to the formation of regular stacking of the silicate layers along the [0 0 1] direction, corresponding to a basal spacing of 0.129 nm, which is normal for montmorillonites [29]. MMT contracted on acidification with the emergence of an A-MMT that yields new peaks at $2\theta \sim 7.7^\circ$ and 16.8° which were absent in MMT.

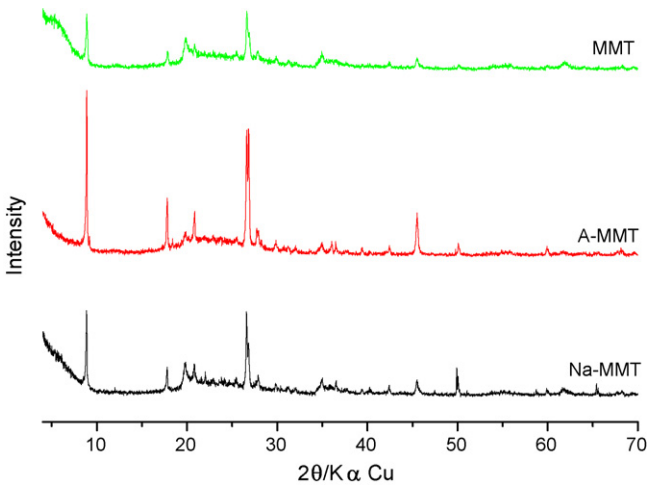

Fig. 1. XRD study of montmorillonites.

These are effects of acid activation which resulted in A-MMT of greater silica content and lower amount of oxides in the octahedral sheet [30]. The peak position of $2\theta = 16.8^\circ$ corresponds to the Si–O–Si layer [31]. Under the hot acid treatment condition, the hydrogen ions attack the aluminosilicate layers of MMT via the interlayer region with several cations (Mg, Al, and Fe) removed from the octahedral sheet. Also some exchangeable Ca^{2+}, Na^+, and K^+, were also removed during the treatment, however, a considerable amount of these elements remained in A-MMT. All these alter the structure, i.e. lead to the destruction of the tetrahedral and octahedral sheets; chemical composition; and physical properties of MMT [32]. For Na-MMT, the interlayer distance of the MMT reference standard increased from 0.126 to 0.184 nm at $2\theta \sim 6.8^\circ$. Changes in the basal spacing depend on the charge, size and hydration behavior of the ion or molecule that is located in the interlayer and on interactions between the ion/molecule and the phyllosilicate layer [33].

The FT-IR spectra (Fig. 2) from the three montmorillonites presented an absorption band at 3705 cm^{-1} corresponding to the stretching of hydroxyls groups and cations from the octahedral sheet. The bending vibrations of water molecule at 2891–3468 cm^{-1} are confirmed by the deformation band at 1701 cm^{-1} with an explanation of reduction in water content due

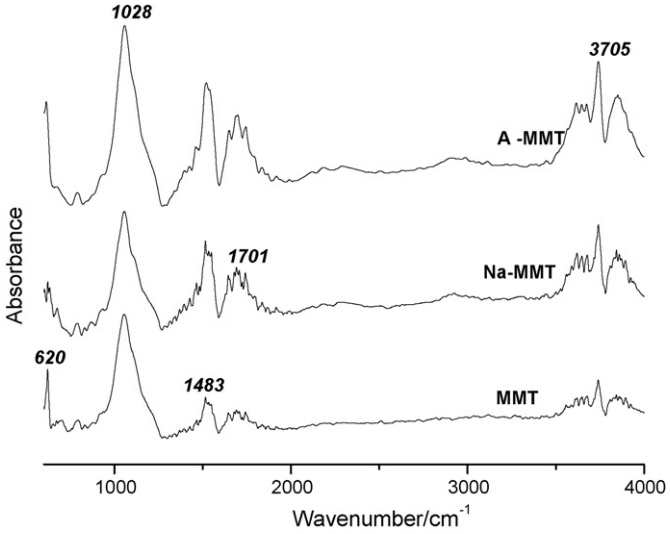

Fig. 2. FT-IR analysis of montmorillonites.

Table 1
BET surface area, pore volume, and pore size of montmorillonites.

Sample	BET surface area (m^2/g)	Pore volume (cm^3/g)	Pore size (nm)
MMT	267.0	0.51	8.44
Na-MMT	285.6	0.54	8.97
A-MMT	190.0	0.36	6.15

to the exchange of H^+ and Na^+ ions with the tetrahedral and octahedral cations during the treatment processes. The bands at 620 cm^{-1} corresponds to deformation vibrations of Si–O–Al [34].

The BET data for the clay samples is presented in Table 1. Considerable changes were recorded in the surface properties of MMT reference standard after treatment with NaCl and acid solutions. The surface area and pore volume of Na-MMT increased and this could be supported by the N_2 adsorption isotherm (Fig. 3). The reduction in surface area and pore volume of A-MMT could be attributed to the concentration of HCl used for the acid activation process. Generally the specific surface area of bentonites increases with increasing severity of acid treatment up to a maximum, and then decreases with further increase in acid concentration. At high acid concentration treatments, the empty spaces grow larger and the micropores are transformed into mesopores. Because of the local decomposition of the crystals, some of the mesopores disappear, leading to a drop in the specific surface area and pore volume [30,34]. The shape of the N_2 adsorption/desorption isotherm at 77 K (Fig. 3) for Na-MMT looks quite similar to that of A-MMT. Nevertheless, more N_2 is being adsorbed by Na-MMT as compared with A-MMT.

4.2. Adsorption studies

4.2.1. Effect of pH

One of the most important factors affecting the removal of heavy metals in wastewater treatment processes is pH [35]. Fig. 4 presents the relationship between the initial pH of Ni^{2+} solution and the percentage removal of Ni^{2+} using Na-MMT and A-MMT. The percentage removal of Ni^{2+} increased with increasing pH values for both adsorbents but Na-MMT displayed a higher removal capability (22–62% removal) as compared to A-MMT (11–58% removal) at all pH values. In montmorillonite–aqueous solution systems, the potential of the surface is determined by the activity of H^+ and OH^- ions (pH), which react with the MMT's surface. For MMT, the potential determining ions are H^+ and OH^- and complex ions formed by the bonding with H^+ and OH^- [10]. At very low pH, the numbers of H_3O^+ ions exceeds

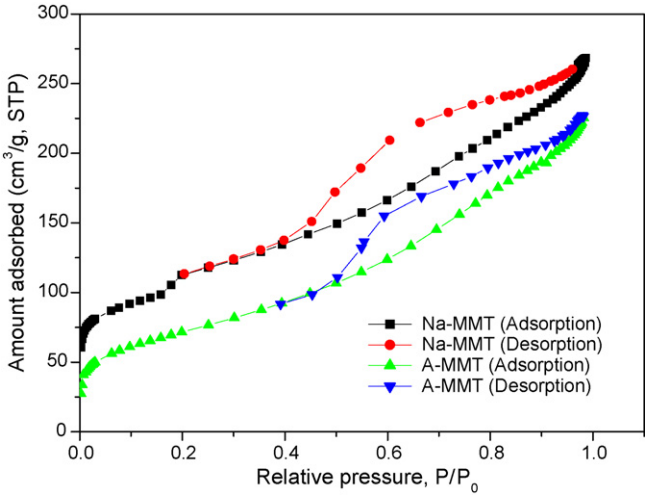

Fig. 3. Nitrogen adsorption/desorption isotherms on Na-MMT and A-MMT at 77 K.

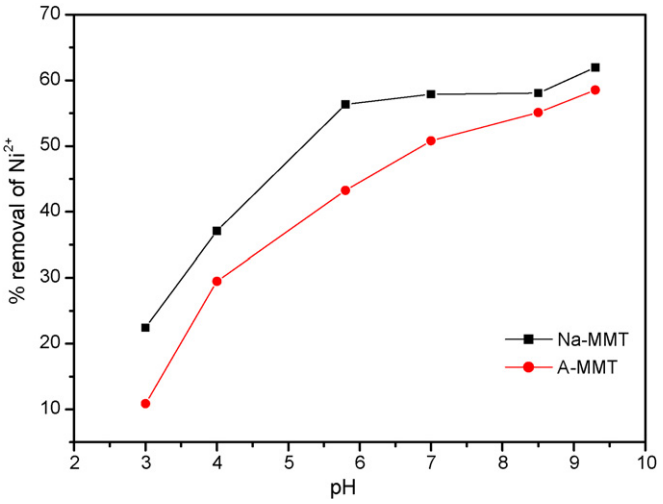

Fig. 4. Effect of pH on Ni^{2+} adsorption (Ni^{2+} concentration, 100 mg/L; adsorbent dose, 6 g/L; equilibrium time, 300 min; temperature 25 ± 0.1 °C; 200 rpm).

that of Ni^{2+} ions and thus compete with Ni^{2+} ions for the binding sites on Na-MMT and A-MMT. The surfaces of Na-MMT and A-MMT remain covered with H_3O^+ ions, Ni^{2+} ions are compelled to remain in liquid-phase. With an increase in pH, the concentration of H_3O^+ ions decreases and some sites become available to Ni^{2+} ions. With continuous decease in acidity more and more sites become available for Ni^{2+} and when pH turns alkaline, precipitation of insoluble nickel-hydroxides may add to higher Ni^{2+} removal from solution. This happens at an approximate pH of 9 for Ni^{2+} [28,36].

The effect of pH on the adsorption of Ni^{2+} onto Na-MMT and A-MMT may be explained on the basis of aqua complex formations of the oxides present in Na-MMT and A-MMT. It has been reported that the pH dependent adsorption of Ni^{2+} on montmorillonite imply that surface complexation contributes mainly to Ni^{2+} adsorption and the following equations may be the main reactions [9,28,36–39]. Exchange which involves hydrated Ni^{2+} can be represented by:

(I) Exchange with hydronium ions:

$$2{\equiv}M\text{–}OH + Ni^{2+} \rightarrow ({\equiv}M\text{–}O)_2Ni + 2H^+ \quad (23)$$

(II) Exchange with Na^{2+} ions at Na-MMT and A-MMT surfaces:

$$2{\equiv}M\text{–}ONa + Ni^{2+} \rightarrow ({\equiv}M\text{–}O)_2Ni + 2Na^+ \quad (24)$$

The exchange of Ni^{2+} with -H or -Na ions at the surfaces of Na-MMT and A-MMT is considered the main method of Ni^{2+} adsorption at pH 6. This surface positive charge is responsible for preventing Ni^{2+} from approaching Na-MMT and A-MMT surfaces and explains the smaller extent of adsorption at low pH.

(III) Hydrolysis of Ni^{2+} in solution:

$$Ni^{2+} + {}_nH_2O \rightarrow Ni(OH)_m(H_2O)_{n-m}^{2-m} + mH^+ \quad (25)$$

(IV) Being $n > m$, and to exchange with hydrolysed species of Ni^{2+}:

$${\equiv}M\text{–}ONa + Ni(OH)_m(H_2O)_{n-m}^{2-m} \rightarrow M\text{–}ONiOH + Na^+ \quad (26)$$

At different pH values, the hydroxylated surface groups vary due to protonation/deprotonation processes as expressed below:

$${\equiv}MOH + H^+ \leftrightarrow MOH_2{}^+ \quad (27)$$

$${\equiv}MOH \leftrightarrow MO^- + H^+ \quad (28)$$

where ≡M may be Al or Si. With increase in pH values, the concentrations of surface species (≡MOH uncharged surface groups;

$\equiv MO_2^+$ positively charged surface groups; $\equiv MO^-$ negatively charged surface groups) become different. The concentration of $\equiv MO_2^+$ decreases with increase in pH, whereas $\equiv MO^-$ increases with increase in pH. The layered structures of Na-MMT or A-MMT would normally expand and become strongly hydrated in the presence of water, resulting in a hydrophilic environment at their surfaces with the Si and the Al metal oxides forming metal–hydroxide complexes. The subsequent acidic or basic dissociation of these complexes at the solid–solution interface may lead to the development of a positive or negative charge on the surface. Ni^{2+} in the solution then drives away a cation on the surface of any negatively charged external surface of Na-MMT or A-MMT. This process continues until all the Ni^{2+} ions are attached to Na-MMT or A-MMT surface and as such, Ni^{2+} replaces the cations of the interlayers in either Na-MMT or A-MMT. With increase in pH, the surface sites becomes more free for the adsorption of Ni^{2+}, $Ni(OH)^+$, $Ni(OH)_2$, $Ni(OH)_3$, $Ni(OH)_4$ and some other Ni-species.

Sodium salts, when used to synthesize MMT, do result in MMT products with large cavities and channels: large cations such as Na^+ and K^+ act as templates around which the aluminosilicate polymerizes, improving the pore properties and enhancing the cation-exchange capacity, hence leading to greater Ni^{2+} uptake in Na-MMT as compared to A-MMT. Also, the retention of the basic MMT structure by Na-MMT, which has high surface charge resulting from the spread of the isomorphous substitution in the tetrahedral and octahedral sheets may have accounted for increase in Ni^{2+} adsorption on Na-MMT. On acidification, the basal spacing of MMT contracted. Exchangeable cations were replaced by protons, followed by partial dissolution of both the octahedral and tetrahedral sheets which creates new acid sites in the structure. The formation of new weaker Si–OH and A1–OH bonds might have also caused dehydroxylation, which all together contributes to a lesser Ni^{2+} adsorptive capacity for A-MMT as compared to Na-MMT. The little difference of Ni^{2+} adsorption on Na-MMT and A-MMT suggests that both adsorbents have very similar adsorption/complexation ability with Ni^{2+}.

4.2.2. Effect of initial concentration

The sorption of Ni^{2+} for both Na-MMT and A-MMT increased with increase in initial Ni^{2+} concentration (Fig. 5). Increasing concentration gradient, acts as increasing the driving force, and in turn leads to an increase in equilibrium sorption until sorbent saturation is reached. Also from Fig. 5, the percentage removal decreases with increase in initial concentration. This may be explained by the fact that at low concentrations, few Ni^{2+} ions are available for the sorption sites, thus, almost all the ions were sorbed. Further increase in concentration of Ni^{2+} led to the saturation of sorbent surface [35]. At all initial Ni^{2+} concentrations studied, Na-MMT has higher percentage removal, e.g. 90% at 50 mg/L as compared to 55% removal for A-MMT at same concentration.

4.2.3. Effect of reaction time

Adsorption processes have been characterized to be very fast physico-chemical reactions [5,6]. Premised on this, time dependence experiments were carried out to understand and investigate the adsorption performance of Na-MMT and A-MMT for Ni^{2+} uptake. Maximum uptake of Ni^{2+} (Fig. 6) was achieved with Na-MMT and A-MMT between 210 and 300 min. Based on this, a reaction time of 300 min was chosen for subsequent studies. The sorption behaviors of Na-MMT and A-MMT fit to the patterns of other natural and modified clay for heavy metals adsorption [5–9,17,31,35,38].

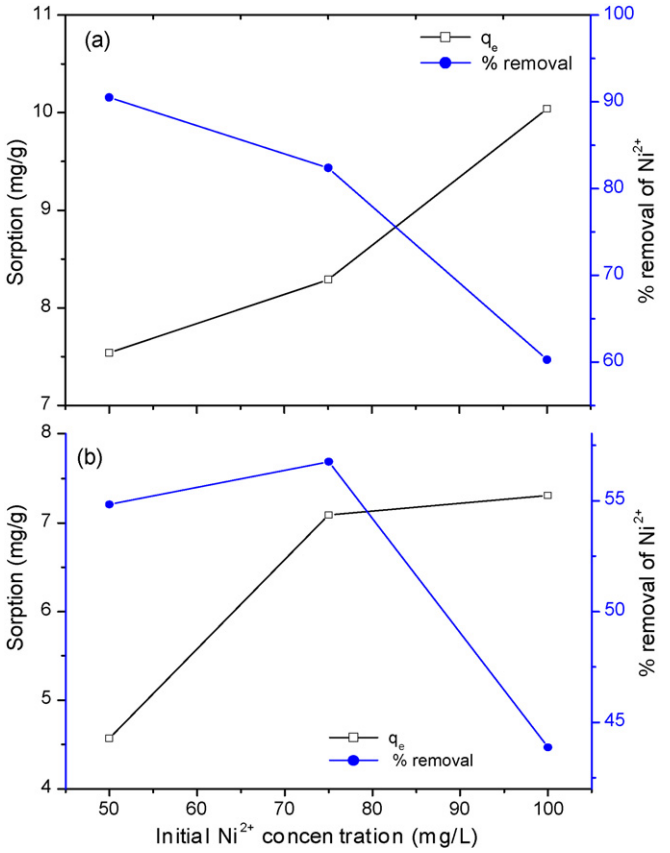

Fig. 5. Effect of initial concentration on adsorption of Ni^{2+} onto (a) Na-MMT and (b) A-MMT (adsorbent dose, 6 g/L; reaction time, 300 min; pH, 6.5 ± 0.1; temperature 25 ± 0.1 °C; 200 rpm).

4.3. Equilibrium isotherm models

The Freundlich model yielded n_F values above unity (Table 2) but may not be appropriate for the description of Ni^{2+} equilibrium sorption onto A-MMT though it has a favorable linearity for Na-MMT equilibrium data, hence it is necessary to analyze the data set to confirm the best fit isotherm for the sorption system. Therefore, the values of standard deviation (S.D.) for each isotherm and

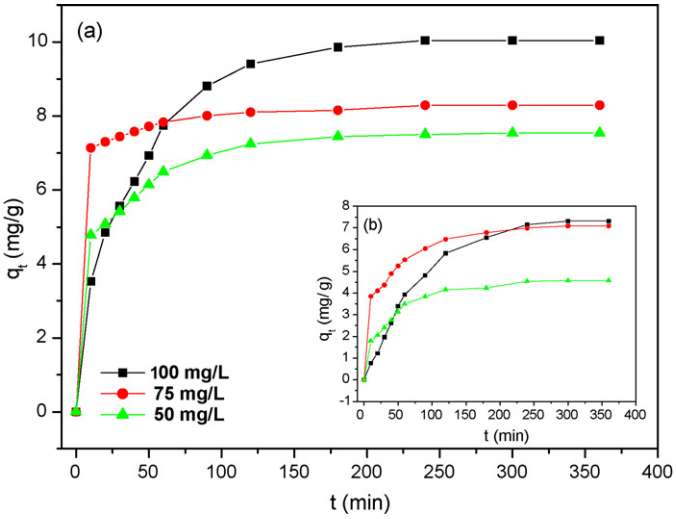

Fig. 6. Time-dependent adsorption of Ni^{2+} onto (a) Na-MMT and (b) A-MMT (Ni^{2+} concentration, 100 mg/L; adsorbent dose, 6 g/L; pH, 6.5 ± 0.1; temperature 25 ± 0.1 °C; 200 rpm).

Table 2
Equilibrium isotherm model parameters for Ni^{2+} sorption onto Na-MMT and A-MMT.

Equilibrium models	Parameters	Na-MMT	A-MMT
Freundlich	K_F ((mg/g)(L/mg)$^{1/n}$)	6.016	1.136
	n_F	7.353	2.092
	q_e Cal. (mg/g)	9.926	7.78
	R^2	0.9854	0.8347
	S.D.	0.035	0.204
Langmuir	Q_m (mg/g)	10.65	11.02
	B (L/mg)	0.362	0.0382
	q_e Cal. (mg/g)	9.96	7.51
	R^2	0.9987	0.9218
	S.D.	0.124	0.929
Tempkin	A_T	108.48	0.277
	b_T (kJ/mol)	2.096	0.885
	q_e Cal. (mg/g)	9.892	7.677
	R^2	0.9789	0.8425
	S.D.	0.370	1.159
Dubinin–Radushkevich	Q_{DR} (mg/g)	9.345	8.566
	E (kJ/mol)	0.705	0.099
	q_e Cal. (mg/g)	9.380	9.446
	R^2	0.8279	0.9420
	S.D.	0.115	0.124
Florry–Huggins	λ	2.506	2.840
	K_{FH}	0.021	0.047
	R^2	0.9691	0.8594
	S.D.	0.083	0.145
Redlich–Peterson	K_R	9.76	3.78
	A_{RP}	0.031	0.014
	β	0.997	0.766
	q_e Cal. (mg/g)	10.08	7.85
	R^2	1.000	0.8497
	S.D.	0.000	0.249

kinetic models were obtained [26] and are given in Tables 2 and 3. If the data from the model is similar to the experimental data, S.D. will be a small number, if it is different, S.D. will be a large number. It was observed from Table 2 that in simulation, the equilibrium data for Na-MMT was best represented by Redlich–Peterson model, which had earlier been reported by [22] to provide better fit than the two-isotherm-parameter models; provided that β value is within the range from 0 to 1. The Redlich–Peterson constant β seems approaching unity, hence, may suggest that the isotherm is approaching Langmuir than Freundlich [40]. There was a good agreement between q_e Exp. (10.04 mg/g) and q_e Cal. (10.08 mg/g) values from the Redlich–Peterson equation. Considering the q_e, R^2 and S.D. values for Na-MMT in Table 2, it can also be said that the Freundlich and the Langmuir equations agree well with the experimental data. Freundlich n_F values being higher than unity for the two adsorbents, indicated that Ni^{2+} was favourably adsorbed by Na-MMT and A-MMT [41]. This type of behavior has also been reported by Tahir and Rauf [42]. According to Chang et al. [43] and Potgieter et al. [44], Ni^{2+} sorption onto Na-rectorite and palygorskite could as well be described by Freundlich model. However, the higher R^2 value of Langmuir when compared with that of the Freundlich, confirms the monolayer coverage of Ni^{2+} onto Na-MMT particles and also the homogeneous distribution of active sites on Na-MMT, as Langmuir equation assumes that adsorbent surface is homogeneous. The Langmuir isotherm was found to be linear for Na-MMT and A-MMT over the entire concentration range studied. Na-MMT presents a better R^2 value (0.9987) to A-MMT (0.9218). The A-MMT equilibrium data followed the D–R model which describes sorption on both homogeneous and heterogeneous surfaces. The S.D. value from this model gives the smallest value as compared to S.D. values from other models (Table 2). The monolayer adsorption capacity of A-MMT (11.02 mg/g) was greater compared with that of Na-MMT (10.65 mg/g) for Ni^{2+} uptake, this may be explained by the partial dissolution of the tetrahedral and octahedral sheets which create the micropore filling of Ni^{2+} ions in the adsorption space within A-MMT pores and therefore, enhancing its monolayer adsorption capacity. Also from Table 2, it can be said that Na-MMT equilibrium data fits the experimental data quite well than A-MMT, nevertheless, both Na-MMT and A-MMT are potential adsorbents for Ni^{2+}.

The R^2 values for Na-MMT and A-MMT using Tempkin model were not as good as the Freundlich and the Langmuir (Table 2), the model when compared for the two adsorbents, seems favorable for Na-MMT with a Tempkin linearity of 0.9789–0.8425 for A-MMT. D–R model adsorption capacities of 9.345 and 8.566 mg/g with E values of 0.705 and 0.099 kJ/mol were obtained for Na-MMT and A-MMT, respectively. Florry–Huggins isotherm was not fit to depict the uptake of Ni^{2+} by both adsorbents, as the R^2 values were 0.9691 and 0.8594 for Na-MMT and A-MMT, respectively.

4.4. Adsorption kinetics

The correlation coefficients for the first-order kinetic model obtained at all the studied concentrations were relatively high for both Na-MMT and A-MMT and it was observed that the pseudo first-order model has an appropriate relation to explain the sorption rate of Ni^{2+} onto Na-MMT and A-MMT considering the small S.D. values in Table 3, but the calculated q_e values at all studied concentrations do not give reasonable values when compared to the experimental q_e values, this makes a confusion, nevertheless, the reactions may not likely to have obeyed the pseudo first-order kinetic though the model presents high R^2 values for both Na-MMT and A-MMT [45]. It is clear from the accuracy of the pseudo second-order model (Table 3) that the adsorption of Ni^{2+} onto Na-MMT and A-MMT can be described by the pseudo second-order chemical reaction and that this reaction significantly controls the adsorption rate of the process [25]. The calculated q_e values agree very well with the experimental data and R^2 values at all concentrations were above 0.998, i.e. close to 1 which indicated that the experimental data can be fitted very well by the pseudo second-order model. Similar result was reported by Fan et al. [31] during a study of Ni^{2+} adsorption onto ACT-attapulgite. The adsorption of Ni^{2+} might have taken place via surface exchange reactions until the surface functional sites were fully occupied; thereafter Ni^{2+} molecules diffuse into the Na-MMT and A-MMT layers for further interactions and/or reactions such as ion-exchange and complexation [35,38,39]. Values for τ (Table 3) obtained from the Elovich model, suggested that the model can be used to explain the heterogeneous surface of Na-MMT and A-MMT since MMT possess active heterogeneous surface sites such as Al_2O_3 and SiO_2, while the values of α may also tell that chemisorption reaction occurred [26]. The R^2 values for the Elovich model were lower than that of the pseudo second-order.

The intraparticle diffusion model showed that the plots of q_t vs. $t^{1/2}$ in Fig. 7 were multi-linear in nature, Webber and Morris [27] reported that if intraparticle diffusion is involved in the adsorption process, the plot of the square root of time vs. adsorption amount would result in a linear relationship, and that, intraparticle diffusion would be the controlling step if this line passes through the origin. Fig. 7 was drawn to test whether the observed sorption is controlled by intraparticle diffusion. The plots do not pass through the origin but show similar features of three separate linear portions for all the concentrations studied. The first portion is attributed to mass transfer effects (slope $k_{id}1$) taking place with boundary layer diffusion while the final linear parts indicate intraparticle diffusion (slope $k_{id}2$ and $k_{id}3$). According to Dal Bosco et al. [7], the major differences between these three portions are given by their slope. While the first presents a pronounced slope, the seconds shows a minor (negligible) slope while the third process shows no slope. These results portray that exchange sites are located on a surface readily accessible to the exchange ions, either at external

Table 3
Kinetic model parameters for the sorption of Ni^{2+} onto Na-MMT and A-MMT.

Kinetic models	Parameters	Na-MMT			A-MMT		
		Concentration of Ni^{2+} solution (mg/L)					
		50	75	100	50	75	100
Pseudo first-order	k_1	0.020	0.018	0.022	0.018	0.016	0.015
	q_e Cal. (mg/g)	5.04	7.84	9.75	3.77	5.44	8.32
	R^2	0.988	0.860	0.998	0.972	0.978	0.979
	S.D.	0.250	0.624	0.071	0.341	0.187	0.173
Pseudo second-order	k_2 (g/mg min)	0.0115	0.0330	0.0038	0.0076	0.0073	0.00091
	q_e Cal. (mg/g)	7.81	8.37	10.18	4.95	7.47	7.61
	R^2	0.999	0.999	0.999	0.999	0.999	0.999
	S.D.	0.302	0.109	0.415	0.930	0.487	1.881
Elovich	α (g/mg min)	1.73	1.70	1.30	0.71	3.13	0.0087
	τ (mg/g)	1.12	2.81	0.50	1.13	0.949	0.47
	q_e Cal. (mg/g)	6.74	9.64	10.91	3.26	6.07	7.18
	R^2	0.975	0.985	0.987	0.981	0.984	0.988
	S.D.	0.238	0.072	0.506	0.204	0.219	0.392
Intraparticle	$k_{id}1$ (mg/g $min^{1/2}$)	0.122	0.429	0.783	0.285	0.334	0.584
	$k_{id}2$ (mg/g $min^{1/2}$)	0.118	0.204	0.384	0.259	0.311	0.343
	$k_{id}3$ (mg/g $min^{1/2}$)	0.020	0.031	0.036	0.046	0.052	0.058
	q_e Cal. (mg/g)	7.03	7.95	10.13	3.98	5.82	7.61
	R^2	0.978	0.987	0.987	0.981	0.984	0.989
	S.D.	1.257	1.811	1.335	0.555	0.968	0.648
Experimental	q_e Exp. (mg/g)	7.54	8.29	10.04	4.57	7.09	7.31

or expanded interlayer surfaces. Hence, these data suggest a limited contribution of mass transfer and boundary layer diffusion in the adsorption process of Ni^{2+} onto Na-MMT and A-MMT and that intraparticle diffusion plays significant role in the adsorption process [46]. The k_{id} values for each initial concentration are given in Table 2. The R^2 values for the diffusion rate parameters $k_{id}1$, $k_{id}2$ and $k_{id}3$ were between 0.978 and 0.989.

4.5. Thermodynamics

The distribution coefficient (K_D) values increase with rise in temperature (Fig. 8). This may infer that more efficient sorption of Ni^{2+} may occur at high temperature [41]. The values of ΔH and ΔS were calculated from the slope and intercept of the plot of $\ln K_D$ against $1/T$ (Fig. 9) using the Eq. (19) [28]. The calculated values are given in Table 4. The values of ΔH are positive for Na-MMT and A-MMT, i.e. endothermic, the possible explanation of the endothermic nature of the enthalpy of adsorption could be based on the well-known fact that ions like Ni^{2+} are well solvated in water [42]. These ions are to some extent denuded of their hydration sheath in order for them to be adsorbed. This dehydration process of ions requires energy and also the removal of water from ions is essentially an endothermic process, and it appears that the endothermicity of the desolvation process exceeds that of the enthalpy of adsorption by a considerable extent. The negative Gibbs free energy change (ΔG) accompanied with positive entropy changes (ΔS) implied that the sorption reactions of Ni^{2+} with Na-MMT and A-MMT are spontaneous with high affinity of Ni^{2+}. Adsorption of Ni^{2+} onto Na-MMT and A-MMT become more favorable at higher temperatures. Similar behavior has been reported for Ni^{2+} sorption onto illite, GMZ bentonite, Na-attapulgite, Na-rectorite and ACT-graft attapulgites, respectively [36,38,41,43,47].

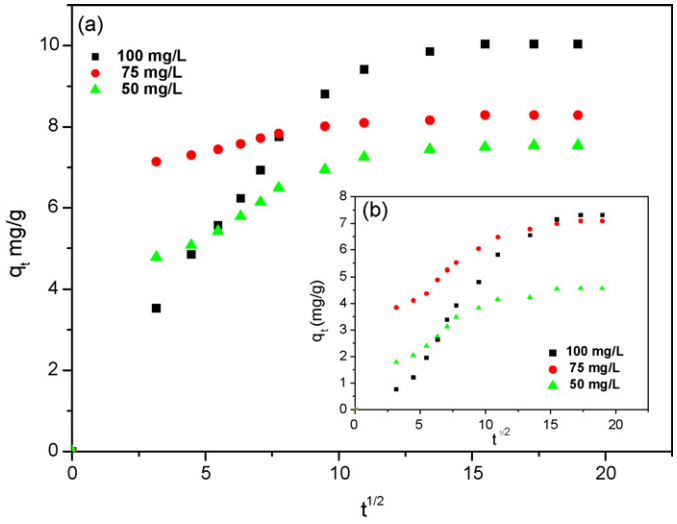

Fig. 7. Webber–Morris plots for adsorption of Ni^{2+} onto (a) Na-MMT and (b) A-MMT (adsorbent dose, 6 g/L; pH, 6.5 ± 0.1; reaction time, 300 min; temperature 25 ± 0.1 °C; 200 rpm).

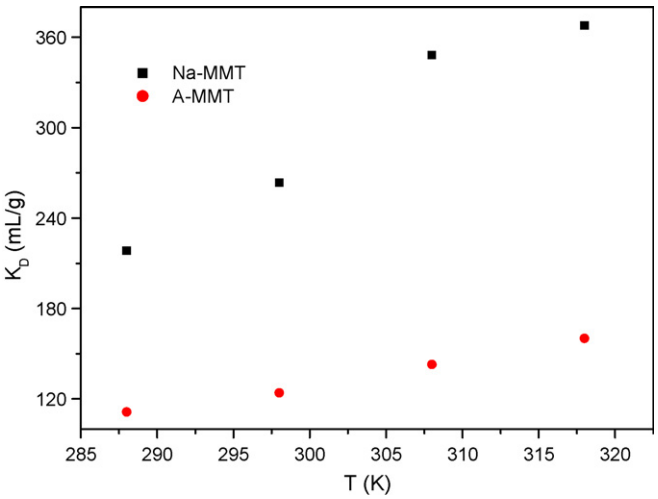

Fig. 8. Plot of distribution coefficient $K_{(D)}$ against temperature for adsorption of Ni^{2+} onto Na-MMT and A-MMT (Ni^{2+} concentration, 100 mg/L; adsorbent dose, 6 g/L; pH, 6.5 ± 0.1; reaction time, 300 min; temperature 25 ± 0.1 °C; 200 rpm).

Table 4
Thermodynamic parameters for the sorption of Ni^{2+} onto Na-MMT and A-MMT.

Adsorbent Ni^{2+}	Temp. (K)	ΔG° (kJ/mol)	ΔH° (kJ/mol)	ΔS° (J/mol K)
Na-MMT	288	−12.92	14.07	93.73
	298	−13.86		
	303	−14.80		
	313	−15.74		
A-MMT	288	−11.26	9.36	71.63
	298	−11.98		
	303	−12.69		
	313	−13.41		

Table 5
Three cycles of Ni^{2+} adsorption–desorption using 0.1 M HCl as desorbing agent.

Adsorbent	No. of cycles	Adsorption, mg/g (%)	Desorption, mg/g (%)
Na-MMT	1	10.01 (60.3)	9.89 (58.7)
	2	9.92 (58.0)	9.64 (55.3)
	3	9.68 (54.6)	9.25 (50.4)
A-MMT	1	7.33 (43.9)	7.21 (42.1)
	2	7.26 (41.7)	6.98 (38.7)
	3	7.05 (38.4)	6.62 (34.2)

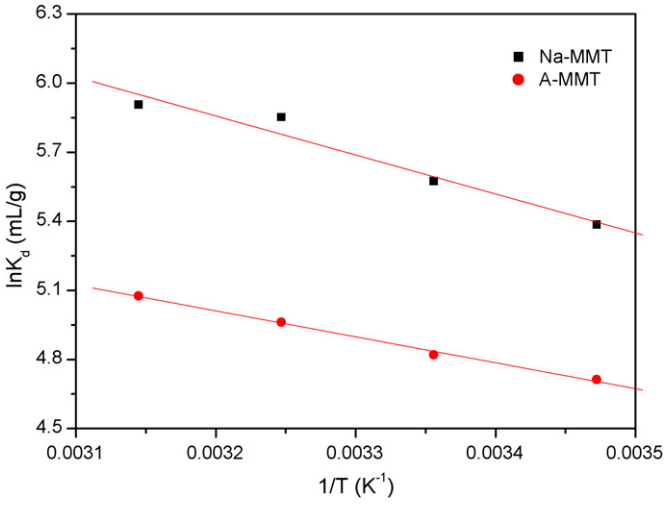

Fig. 9. Plots of $\ln K_{(D)}$ vs. $1/T$ for Ni^{2+} adsorption onto Na-MMT and A-MMT (Ni^{2+} concentration, 100 mg/L; adsorbent dose, 6 g/L; pH, 6.5 ± 0.1; reaction time, 300 min; temperature 25 ± 0.1 °C; 200 rpm).

4.6. Desorption and regeneration studies

To make the adsorption process more economical, it is necessary to regenerate the spent adsorbent. Therefore, the result of the desorption test carried on spent Na-MMT and A-MMT using 0.1 M HCl solution is presented in Table 5. After three cycles, the sorption capacity of the Na-MMT and A-MMT decreased from 60.3% to 54.6% and 43.88% to 38.38%, respectively. The recovery of Ni^{2+} by 0.1 M HCl decreases from 58.7% in the first cycle to 50.4% in the third cycle for Na-MMT while that of A-MMT decreased from 42.1% in the first cycle to 34.2% in the third cycle. H^{+} may replace Ni^{2+} on the metal loaded Na-MMT and A-MMT adsorbents thus functioning as a cation exchanger.

5. Conclusion

Sodium exchanged (Na-MMT) and acid modified montmorillonite (A-MMT) without calcinations are capable of removing Ni^{2+} from aqueous solution. The percentage removal of Ni^{2+} increased with increase in pH for both adsorbents. Na-MMT displayed higher removal capability (22–62% removal) as compared to A-MMT (11–58% removal). Maximum adsorbed amount of Ni^{2+} was achieved for both Na-MMT and A-MMT within 210–300 min. From linear forms of the equilibrium sorption isotherm models, Na-MMT satisfactorily fit the models in the order: Redlich–Peterson > Langmuir > Freundlich > Tempkin > Florry – Huggins > Generalized > Dubinin–Radushkevich model while the trend for A-MMT is, Dubinin–Radushkevich > Langmuir > Florry–Huggins > Redlich–Peterson > Generalized > Tempkin > Freundlich. The pseudo second-order model best described the adsorption kinetics of Ni^{2+} onto Na-MMT and A-MMT based on the assumption that the rate-limiting step may be chemical sorption or chemisorption involving valence forces through sharing or exchange of electrons between Ni^{2+} and the adsorbents. The thermodynamic studies revealed an increase in Ni^{2+} uptake, with increase in temperature. This implies, sorption of Ni^{2+} requires a diffusion process, which is basically an endothermic process. The negative values of ΔG° obtained for Na-MMT and A-MMT indicated a spontaneous nature of Ni^{2+} sorption onto Na-MMT and A-MMT. The spent adsorbents can be regenerated and reused upon treatment with acid and the potentials of un-calcined Na-MMT and A-MMT can be explored as effective adsorbents for Ni^{2+} removal in aqueous solutions.

Acknowledgements

The authors appreciate the supports of the Schlumberger Stiching Fund, the ERC program of the National Research Foundation (NRF), Korea and the Korea Institute of Geoscience and Mineral Resources (KIGAM) towards this project.

References

[1] P.T. Anastas, M.M. Kirchhoff, Origins, current status, and future challenges of green chemistry, Acc. Chem. Res. 35 (2002) 686–694.
[2] S.P. Parker, Encyclopedia of Environmental Science, second ed., McGraw-Hill, New York, 1980.
[3] K. Kadirvelu, K. Thamaraiselvi, C. Namasivayam, Adsorption of nickel (II) from aqueous solution onto activated carbon prepared from coirpith, Sep. Purif. Technol. 24 (2001) 497–505.
[4] R.P. Beliles, The lesser metals, in: F.W. Oehme (Ed.), Toxicity of Heavy Metals in the Environment. Part 2, Marcel Dekker, New York, 1979, pp. 547–616.
[5] K.G. Bhattacharyya, S.S. Gupta, Adsorption of few heavy metals on natural and modified kaolinite and montmorillonite: a review, Adv. Colloids Interface Sci. 140 (2008) 114–131.
[6] S.E. Bailey, J. Trudy, T.J. Olin, M.R. Bricka, D.D. Adrian, A review of potentially low cost sorbents for heavy metals, Water Res. 33 (1999) 2469–2479.
[7] S.M. Dal Bosco, R.S. Jimenez, C. Vignado, J. Fontana, B. Geraldo, F.C.A. Figueiredo, D. Mandelli, W.A. Carvalho, Removal of Mn(II) and Cd(II) from

wastewaters by natural and modified clays, Adsorption 12 (2006) 133–146.
[8] C.O. Ijagbemi, M.H. Baek, D.S. Kim, Montmorillonite surface properties and sorption characteristics for heavy metal removal from aqueous solutions, J. Hazard. Mater. 166 (2009) 538–546.
[9] H. Marcussen, P.E. Holm, B.W. Strobel, H.C.B. Hansen, Nickel sorption to goethite and montmorillonite in presence of citrate, Environ. Sci. Technol. 43 (2009) 1122–1127.
[10] Bergaya, B.K.G. Theng, G. Lagaly, Handbook of Clay Science, first ed., Elsevier, 2006.
[11] R. Francisco, D. Valenzuela, S. Persio de Souza, Studies on the acid activation of Brazilian smectitic clays, Quimica Nova 24 (2001) 345–353.
[12] P. Kumar, R.V. Jasra, T.S.G. Bhat, Evolution of porosity and surface acidity in montmorillonite clay on acid activation, Ind. Eng. Chem. Res. 34 (1995) 1440–1448.
[13] S. Dultz, J. Bors, Organophilic bentonites as adsorbents for radionuclides. II. Chemical and mineralogical properties of HDPy–montmorillonite, Appl. Clay Sci. 16 (2000) 15–29.
[14] Standard Methods for Examination of Water and Wastewater, twentieth ed., APHA, AWWA, Washington, DC, New York, 1998.
[15] J. Rodier, Water Analysis, seventh ed., Dunod, Paris, 1996 (in French).
[16] H. Freundlich, Adsorption in solution, Phys. Chem. Soc. 40 (1906) 1361–1368.
[17] S. Veli, B. Alyuz, Adsorption of copper and zinc from aqueous solutions by using natural clay, J. Hazard. Mater. 149 (2007) 226–233.
[18] I. Langmuir, The adsorption of gases on plane surfaces of glass, mica and platinum, J. Am. Chem. Soc. 40 (1918) 1361–1403.
[19] M.J. Temkin, V. Pyzhev, Recent modifications to Langmuir isotherms, Acta Physiochim. URRS 12 (1940) 217–222.
[20] M.M. Dubinin, The potential theory of adsorption of gases and vapours for adsorbents with energetically non-uniform surfaces, Chem. Rev. 60 (1960) 235–266.
[21] M. Polanyi, Theories of the adsorption of gases. A general survey and some additional remarks, Trans. Faraday Soc. 28 (1932) 316–332.
[22] O. Redlich, D.L. Peterson, A useful adsorption isotherm, J. Phys. Chem. 63 (1959) 1024–1102.
[23] M. Horsfall, A.I. Spiff, Equilibrium sorption study of Al^{+3}, Co^{+2} and Ag^{+} in aqueous solution by fluted Pumpkin (*Telfairia Occidentalis Hook*) waste biomass, Acta Chim. Slov. 52 (2005) 174–181.
[24] S. Lagergren, About the theory of so called adsorption of soluble substance, Kungliga svenska ertenskapsakademiens, Hand Linger 24 (1898) 1–39.
[25] Y.S. Ho, G. McKay, Pseudo-second order model for sorption process, Process Biochem. 34 (1999) 451–465.
[26] E. Bulut, M. Özacar, İ.A. Şengil, Equilibrium and kinetic data and process design for adsorption of Congo Red onto bentonite, J. Hazard. Mater. 154 (2008) 613–622.
[27] W.J. Webber, J.C. Morris, Kinetics of adsorption on carbon from solution, J. Sanit. Eng. Div. Am. Soc. Civil Eng. 89 (1963) 31–60.
[28] Q.H. Fan, D.D. Shao, Y. Lu, W.S. Wu, X.K. Wang, Effect of pH, ionic strength, temperature and humic substances on the sorption of Ni(II) to Na-attapulgite, Chem. Eng. J. 150 (2009) 188–195.
[29] R.E. Grim, International Series in Earth and Planetary Sciences, McGraw-Hill, New York, 1953.
[30] E.L. Foletto, C. Volzone, L.M. Porto, Performance of an Argentinian acid-activated bentonite in the bleaching of soyabean oil, Braz. J. Chem. Eng. 20 (2003) 139–145.
[31] Q.H. Fan, D.D. Shao, J. Hu, W.S. Wu, X.K. Wang, Comparison of Ni^{2+} sorption to bare and ACT-graft attapulgites: effect of pH, temperature and foreign ions, Surface Sci. 602 (2008) 778–785.
[32] W.P. Gates, J.S. Anderson, M.D. Raven, G.J. Churchman, Mineralogy of a bentonite from Miles, Queensland, Australia and characterisation of its acid activation products, Appl. Clay Sci. 20 (2002) 189–197.
[33] N.M. Nagy, J. Konya, The adsorption of valine on cation-exchanged montmorillonites, Appl. Clay Sci. 25 (2004) 57–69.
[34] B. Tyagi, C.D. Chudasama, R.V. Jasra, Determination of structural modification in acid activated montmorillonite clay by FT-IR spectroscopy, Spectrochim. Acta Part A 64 (2006) 273–278.
[35] S.S. Gupta, K.G. Bhattacharyya, Adsorption of Ni(II) on clays, J. Colloids Interface Sci. 295 (2006) 21–32.
[36] J. Echeverría, J. Indurain, E. Churio, J. Garrido, Simultaneous effect of pH, temperature, ionic strength, and initial concentration on the retention of Ni on illite, Colloids Surfaces A 218 (2003) 175–187.
[37] G. Montavon, E. Alhajiji, B. Grambow, Study of the interaction of Ni^{2+} and Cs^{+} on MX-80 bentonite; effect of compaction using the "capillary method", Environ. Sci. Technol. 40 (2006) 4672–4679.
[38] D. Xu, X. Zhou, X. Wang, Adsorption and desorption of Ni^{2+} on Na-montmorillonite: effect of pH, ionic strength, fulvic acid, humic acid and addition sequences, Appl. Clay Sci. 39 (2008) 133–141.
[39] X. Gu, L.J. Evans, Surface complexation modelling of Cd(II), Cu(II), Ni(II), Pb(II) and Zn(II) adsorption onto kaolinite, Geochim. Cosmochim. Acta 72 (2008) 267–276.
[40] K.V. Kumar, S. Sivanesan, Comparison of linear and non-linear method in estimating the sorption isotherm parameters for safranin onto activated carbon, J. Hazard. Mater. 123 (2005) 288–292.
[41] X. Tan, C. Chen, S. Yu, X. Wang, Sorption of Ni^{2+} on Na-rectorite studied by batch and spectroscopy methods, Appl. Geochem. 23 (2008) 2767–2777.
[42] S.S. Tahir, N. Rauf, Thermodynamic studies of Ni(II) adsorption onto bentonite from aqueous solution, J. Chem. Thermodyn. 35 (2003) 2003–2009.
[43] P. Chang, X. Wang, S. Yu, W. Wu, Sorption of Ni(II) on Na-rectorite from aqueous solution: effect of pH, ionic strength and temperature, Colloids Surface A: Physicochem. Eng. Aspects 302 (2007) 75–81.
[44] J.H. Potgieter, S.S. Potgieter-Vermaak, P.D. Kalibantonga, Heavy metals removal from solution by palygorskite clay, Miner. Eng. 19 (2006) 463–470.
[45] Y.S. Ho, G. McKay, Batch lead (II) removal from aqueous solution by peat: equilibrium and kinetics, Trans. Inst. Chem. Eng. 77B (1999) 165–173.
[46] P. Trivedi, L. Axe, T.A. Tyson, XAS studies of Ni and Zn sorbed to hydrous manganese oxide, Environ. Sci. Technol. 35 (2001) 4515–4521.
[47] S. Yang, J. Li, Y. Lu, Y. Chen, X. Wang, Sorption of Ni(II) on GMZ bentonite: effects of pH, ionic strength, foreign ions, humic acid and temperature, Appl. Radiat. Isotopes 67 (2009) 1600–1608.